Stability and turbulence in the atmospheric boundary layer: A comparison of remote sensing and tower observations

Katja Friedrich,[1] Julie K. Lundquist,[1,2] Matthew Aitken,[3] Evan A. Kalina,[1] and Robert F. Marshall[1]

Received 28 November 2011; revised 4 January 2012; accepted 9 January 2012; published 8 February 2012.

[1] When monitoring winds and atmospheric stability for wind energy applications, remote sensing instruments present some advantages to *in-situ* instrumentation such as larger vertical extent, in some cases easy installation and maintenance, measurements of vertical humidity profiles throughout the boundary layer, and no restrictions on prevailing wind directions. In this study, we compare remote sensing devices, Windcube lidar and microwave radiometer, to meteorological *in-situ* tower measurements to demonstrate the accuracy of these measurements and to assess the utility of the remote sensing instruments in overcoming tower limitations. We compare temperature and wind observations, as well as calculations of Brunt-Väisälä frequency and Richardson numbers for the instrument deployment period in May–June 2011 at the U.S. Department of Energy National Renewable Energy Laboratory's National Wind Technology Center near Boulder, Colorado. The study reveals that a lidar and radiometer measure wind and temperature with the same accuracy as tower instruments, while also providing advantages for monitoring stability and turbulence. We demonstrate that the atmospheric stability is determined more accurately when the liquid-water mixing ratio derived from the vertical humidity profile is considered under moist-adiabatic conditions. **Citation:** Friedrich, K., J. K. Lundquist, M. Aitken, E. A. Kalina, and R. F. Marshall (2012), Stability and turbulence in the atmospheric boundary layer: A comparison of remote sensing and tower observations, *Geophys. Res. Lett.*, *39*, L03801, doi:10.1029/2011GL050413.

1. Introduction

[2] Wind anemometers and thermometers mounted on a tower have served as a benchmark for meteorological observations at wind farms, despite limited vertical extents, typically 60–100 m. With the height limitation, towers can often not provide the observations required for accurate wind measurements and forecasts, which are needed to satisfy the rapid evolution of new wind turbine technologies. Moreover, tower measurements at wind farms rarely include humidity, which is crucial to determining atmospheric stability under near-saturated conditions. On the other hand, with improvements in spatial and temporal resolution and measurement accuracy, in addition to declining costs, over the last 10 years, most remote sensing instruments can be now considered a viable alternative to in-situ tower instrumentation. There has been considerable uncertainty within the wind energy industry regarding the utility of remote sensing instruments, which this paper seeks to address. In this study, we demonstrate that combining a Windcube lidar with a microwave radiometer provides measurements of wind and temperature comparable to or better than those obtained from tower observations. Furthermore, this combination overcomes the limits of traditional tower measurements by collecting measurements well above tower heights. To our knowledge, this study is the first time these instruments have been deployed and compared in this manner. While the importance of humidity measurements has not yet been quantified for wind farm applications, we demonstrate that atmospheric stability is determined more accurately when the liquid-water mixing ratio derived from the vertical humidity profile is considered when the atmosphere is saturated.

[3] Vertical profiles of moisture are generally not measured by *in-situ* tower instruments for wind farm applications [*AWS Truepower*, 2010]. As a result, buoyancy-driven forcing might not be correctly determined in a saturated atmosphere. The Richardson number (*Ri*) compares the magnitude of buoyancy-driven forcing (also referred to as squared dry Brunt-Väisälä frequency, N_d^2) to shear-driven forcing. In a saturated atmosphere, latent heat affects the temperature profile, and therefore a modification is required to incorporate the change in latent heat from condensation of water vapor [*Einaudi and Lalas*, 1973; *Durran and Klemp*, 1982], namely the squared moist Brunt-Väisälä frequency (N_m^2). To quantify the advantages of remote sensing instruments and the role of humidity on *Ri*, a comparison experiment was conducted between 24 May–16 June 2011 at the Department of Energy's National Renewable Energy Laboratory's (NREL) National Wind Technology Center near Boulder, Colorado. Simultaneous profiles of temperature, moisture, and wind were collected by a Radiometrics MP-3000A microwave radiometer, an NRG/Leosphere Windcube version 1 lidar, and sensors mounted on an 82-m meteorological tower. Section 2 presents the accuracy of wind and temperature measurements from the Windcube lidar and the microwave radiometer compared to *in-situ* tower observations and the influence of the humidity profile on atmospheric stability and Richardson number. Section 3 illustrates the advantages of remote sensing instruments for monitoring atmospheric stability and turbulence intensity in the atmospheric boundary layer. More information about the instruments and on how *Ri*, N_d^2, and N_m^2 are calculated in a

[1]Department of Atmospheric and Oceanic Sciences, University of Colorado at Boulder, Boulder, Colorado, USA.
[2]National Renewable Energy Laboratory, Golden, Colorado, USA.
[3]Department of Physics, University of Colorado at Boulder, Boulder, Colorado, USA.

0094-8276/12/2011GL050413

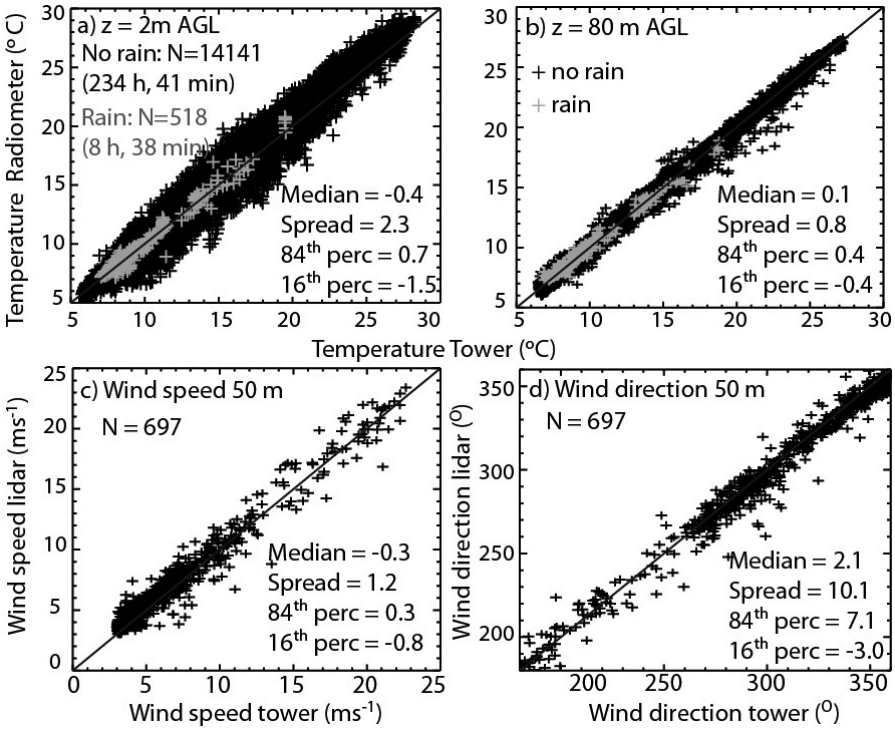

Figure 1. Scatter plot of (a, b) temperature measured by thermometers mounted on a meteorological tower and a microwave radiometer and (c, d) wind speed and direction measured by anemometers mounted on the meteorological tower and the Windcube lidar between 24 May and 16 June 2011.

saturated and unsaturated atmosphere is provided in the auxiliary material.[1]

2. Comparison Between Tower and Remote Sensing Observations

2.1. Temperature and Wind

[4] Comparisons between temperature measurements from the microwave radiometer and the *in-situ* tower observations (Figure 1) provide an assessment of the utility of the radiometer at the altitudes where the tower collected profiles. The temperature from the radiometer was compared to the tower observation taken within a time interval of ± 1 min. Radiometer measurements are available at 50-m increments at 0 m, 50 m, 100 m, etc., and so the temperature "observed" by the radiometer at 2 m and 80 m was interpolated from the 0-m and 50-m and 50-m and 100-m observations, respectively (see auxiliary material). The largest differences in temperature were observed at the surface with a difference between the 16th and 84th percentile (hereafter referred to as spread) of 2.3°C (Figure 1a) and a slight bias of -0.4°C (tower temperature is lower). The large contrast at the surface can be related to differences in sensible heat release or the coarse vertical resolution of the radiometer between 0–50 m compared to point measurements from the tower at 2 m and 50 m, which could prevent the radiometer from resolving temperature inversions close to the surface. The differences in temperature decreased with distance from the surface as indicated by the decrease in spread from 2.3°C at the surface to 1.4°C at 50 m (figure not shown) to 0.8°C at 80 m (Figure 1b). The median in temperature difference remained at ± 0.1°C at 50 m and 80 m.

[5] To compare the tower wind observations with the Windcube lidar measurements, we averaged the tower data at 2 m, 50 m and 80 m over 10 min. Unfortunately, the vane at 80 m AGL was broken during the comparison period, so the wind analysis solely focuses on the measurements at 50 m AGL. Of note, Windcube measurements were accomplished up to 140 m 98.3% of the time during this collection period, and up to 200 m 77.5% of the time, similar to the results found by *Aitken et al.* [2012]. Recognizing that the tower wind speed and direction measurements are only reliable when they are not in the wake of the tower, we only considered westerly flow cases when the wind speed was >3 ms^{-1} (i.e., minimum wind speed for turbines to operate) between 180° and 360° as measured both by the anemometer and the Windcube lidar. The differences in wind speed between the lidar and the anemometer at 50 m AGL were relatively small with a median of -0.3 ms^{-1} and a spread of 1.2 ms^{-1}, as indicated in Figure 1c. The Windcube observed slightly higher wind speeds compared to the anemometer. The comparison of wind direction reveals a median differences of 2.1° and a spread of 10.1° (Figure 1d).

2.2. Brunt-Väisälä Frequency

[6] The 1-minute temperature profiles observed by the radiometer and tower thermometers (between the surface and 80 m AGL) enable calculations of the squared Brunt-Väisälä frequency (see auxiliary material), and therefore, the buoyant forcing between the surface and 80 m AGL (Figure 2a). We calculated frequencies using the same surface temperature measurement from the radiometer because the lowest tower measurement available is at 2 m AGL, and

[1] Auxiliary materials are available in the HTML. doi:10.1029/2011GL050413.

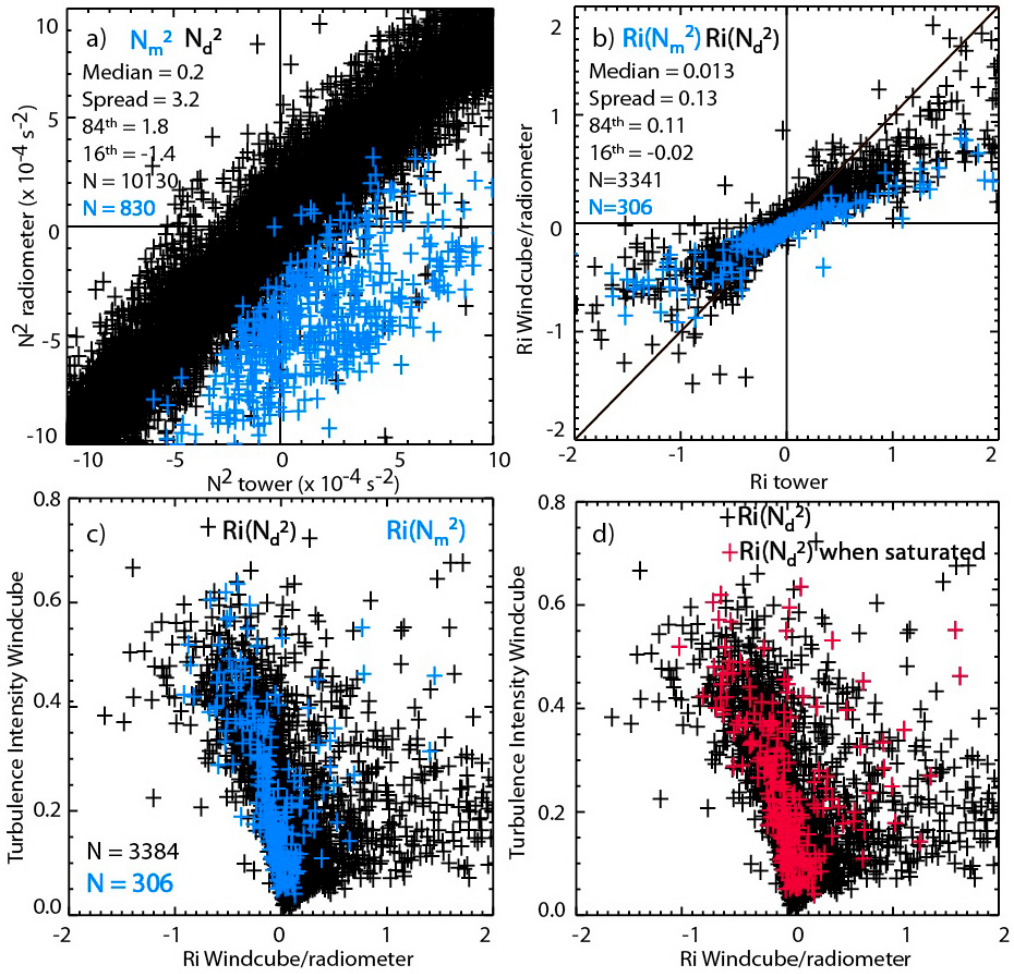

Figure 2. (a) Scatter plot of Brunt-Väisälä frequency for unsaturated (black plus signs) and saturated conditions (blue plus signs) derived from 1-minute temperature observations at the tower and 1-minute temperature and moisture measurements from the radiometer between the surface and 80 m AGL. (b) Scatter plot of *Ri* between the surface and 50 m AGL (black plus signs) measured by the anemometers and Windcube lidar every 10 min. Black plus signs indicate *Ri* values using N_d^2, while blue plus signs represent the Richardson numbers with N_m^2. (c) Turbulence intensity as a function of *Ri* values at 80 m AGL derived from the 10-minute Windcube observations. Blue plus signs represent time steps when the atmosphere was saturation; (d) red plus signs represent the same time steps but using the dry Richardson number.

a large temperature gradient is expected between the surface and 2 m AGL (cf. Figure 1a). The tower and the radiometer tend to agree on the nature of the temperature profile. Only 5.6% of all time periods showed disagreement: 1.3% of the time the radiometer suggested negative N_d^2 values (unstable) while the tower suggested positive N_d^2 values (stable), while 4.3% of the time the radiometer suggested positive N_d^2 values (stable) while the tower suggested negative N_d^2 values (unstable).

[7] To study the impact of latent heat release on atmospheric stability, we calculated N_m^2 and included the vertical profile of moisture from the radiometer during time periods with rain and when the relative humidity was ≥100% either at the surface or at 50 m AGL (8% of the data). During about 34% of the events with a saturated atmosphere (blue plus signs in Figure 2a), the radiometer observations using the moisture profile indicated negative N_m^2 (unstable), while the tower measurements suggested positive N_d^2 (stable).

2.3. Richardson Number

[8] The Richardson number (*Ri*) compares buoyant forcing to shear forcing; negative values indicate an unstable atmosphere while positive values indicate a stable atmosphere. Herein, we calculate *Ri* from vertical profiles of potential temperature observed by the radiometer and the wind observations from the Windcube between the surface and 50 m AGL (see auxiliary material). We assumed the winds were still at the surface ($u = v = 0$ ms^{-1}) following *Vickers and Mahrt* [2004] and *Mahrt* [2010]. We compared *Ri* calculations from the remote sensing instruments to the *Ri* calculations but using *in-situ* tower observations, all averaged over 10-minutes to match the Windcube measurements. As with the wind comparison in Figures 1c and 1d, only winds in excess of 3 ms^{-1} and with wind directions between 180°–360° are considered for the analysis. Differences between the *in-situ* and remote sensing-based *Ri* values have median and spread values of 1.3×10^{-2} and 13×10^{-2}, respectively. The smallest differences occurred

for small *Ri* within stable atmospheric conditions with considerable wind shear, while larger differences occurred when $Ri > 0.3$ (Figure 2b). N_m^2 is included in the *Ri* calculations using the Windcube and radiometer observations when the relative humidity at the surface or at 50 m AGL is ≥100% or rain was observed at the surface (blue plus signs in Figure 2b), which accounts for 6% of the total data. During about 56% of the events using N_m^2, the Richardson numbers, calculated from the remote sensing observations and the moisture profile information, were negative (unstable atmosphere), while the tower measurements indicated a stable atmosphere with positive *Ri*. In most of the cases with a saturated atmosphere, the atmospheric stability would be assessed incorrectly using the tower conditions.

3. Lidar and Radiometer Observations for Wind Farm Applications

3.1. Turbulence Intensity

[9] Performance of wind turbines is also sensitive to changes in atmospheric turbulence, which is a measure of the variation in wind speed about the mean [*Kaiser et al.*, 2003; *Rareshide et al.*, 2009; *Wharton and Lundquist*, 2012; *Vanderwende and Lundquist*, 2012]. Although most researchers prefer to use a three-dimensional assessment of turbulent motions, many wind farms only deploy cup anemometers, so turbulence intensity is often the only available estimate of turbulent motions. Turbulence intensity is defined as the ratio of the standard deviation of the horizontal wind velocity to the mean wind velocity. Low turbulence intensity is expected under stable conditions, while strong mixing during unstable conditions will increase the turbulence intensity. Herein, we calculated the turbulence intensity using wind observations from the Windcube lidar and compare those values to *Ri* in both saturated and unsaturated conditions (Figures 2c and 2d). High values of turbulence intensity were observed when the atmosphere was unstable or neutral with negative Richardson numbers and Richardson numbers close to zero in an unsaturated environment, respectively. With increasing stability, i.e., an increase in *Ri*, the turbulence intensity decreased. In a saturated atmosphere (blue plus signs in Figure 2c), turbulence intensity ranged between 0 and 0.7. Using the dry Richardson number in a saturated atmosphere can lead to inaccuracies, which are linked to high values of turbulence intensity and increasing positive *Ri* numbers. In the limited cases we explored, when *Ri* numbers were close to zero, the relationship between turbulent intensity and *Ri* numbers were similar for a saturated and unsaturated atmosphere.

3.2. Richardson Number During a Cold Front Passage

[10] Figure 3 shows the Windcube and microwave radiometer observations during a cold front passage on 9 June 2011. This case is used to demonstrate the usefulness of combined high-resolution Windcube lidar and microwave radiometer measurements beyond the 80 m AGL tower measurements, when the atmosphere shifts between being unsaturated and saturated. On that day, an upper-level trough passed over Colorado with a surface cold front moving over the instruments at about 0820 UTC. Prior to the cold front passage (0000–0820 UTC), the atmosphere below the mountain crests (∼1 km AGL) was stable with a northerly surface wind of 5–15 ms^{-1} (Figures 3a and 3e). With a relative humidity below 60%, the atmosphere was unsaturated and stable with turbulence intensity values <0.4. During the cold front passage, the surface temperature dropped by ∼10°C (Figure 3b), relative humidity increased from 20% to 100% (Figure 3c), wind veered to the east for ∼1 h and then returned to northwesterly winds with steady wind speeds of 15 ms^{-1} (Figure 3a). During the cold front passage, the atmosphere became neutral with Richardson numbers around zero and remained neutral under both saturated and unsaturated conditions, and turbulence intensity remained below 0.2 between 0820–1130 UTC. Note that N_m^2 was negative, while N_d^2 remained around zero. As a result, the Richardson numbers, which are similar for a saturated and unsaturated atmosphere, were governed by the wind shear. Between 1200–1500 UTC, the atmosphere became slightly conditionally unstable, i.e., slightly stable/neutral if an unsaturated atmosphere are assumed but unstable, when the atmosphere is assumed to be saturated (Figure 3d). Accordingly, turbulence intensity slightly increased and ranged between 0.2–0.6 (Figure 3e). With relative humidity values >95%, the atmosphere was close to saturation during this time. Rain was observed at 0430 UTC prior to the cold front passage and occasionally at the surface between 0820–1430 UTC (Figure 3c). While maintaining the wind speed, the wind direction backed to northerly after 2000 UTC. The atmosphere became more unstable under both saturated and unsaturated conditions.

[11] The calculation of the Brunt-Väisälä frequency and the Richardson number underscore the critical role of latent heat release in understanding atmospheric stability and turbulence. Even though rain only occurred occasionally after 0820 UTC, it can be assumed, based on the low cloud height and the relative humidity exceeding 95%, that the atmosphere was near-saturated. The differences between the Richardson numbers using N_d^2 and N_m^2 increased to ∼0.2 between 0820–1400 UTC. After 1400 UTC, the atmosphere became unstable under both saturated and unsaturated conditions, and *Ri* decreased for both *in-situ* and remote sensing instruments.

[12] The microwave radiometer observations also revealed important meteorological structures, which are important to forecast the 3-dimensional structure of the atmosphere and cannot be observed with tower observations. Prior to the cold front passage, evaporation occurred below 1.5 km AGL, as indicated by a large gradient in relative humidity. Upper-level dry-air intrusions, which occurred after 1300 UTC above 1 km AGL, have been often been observed with the passage of an upper-level trough leading to a destabilization of the atmosphere [*Steenburgh*, 2003; *Colle et al.*, 2005].

4. Conclusion

[13] We examined the advantages of remote sensing of turbulence and stability within the atmospheric boundary layer by comparing Windcube lidar and microwave radiometer measurements to *in-situ* tower observations. The investigation focused on three main issues: 1) the accuracy of wind and temperature measurements from the remote sensing instruments, 2) advantages of remote sensing instruments for monitoring stability and turbulence in the atmospheric boundary layer, and 3) the influence of the

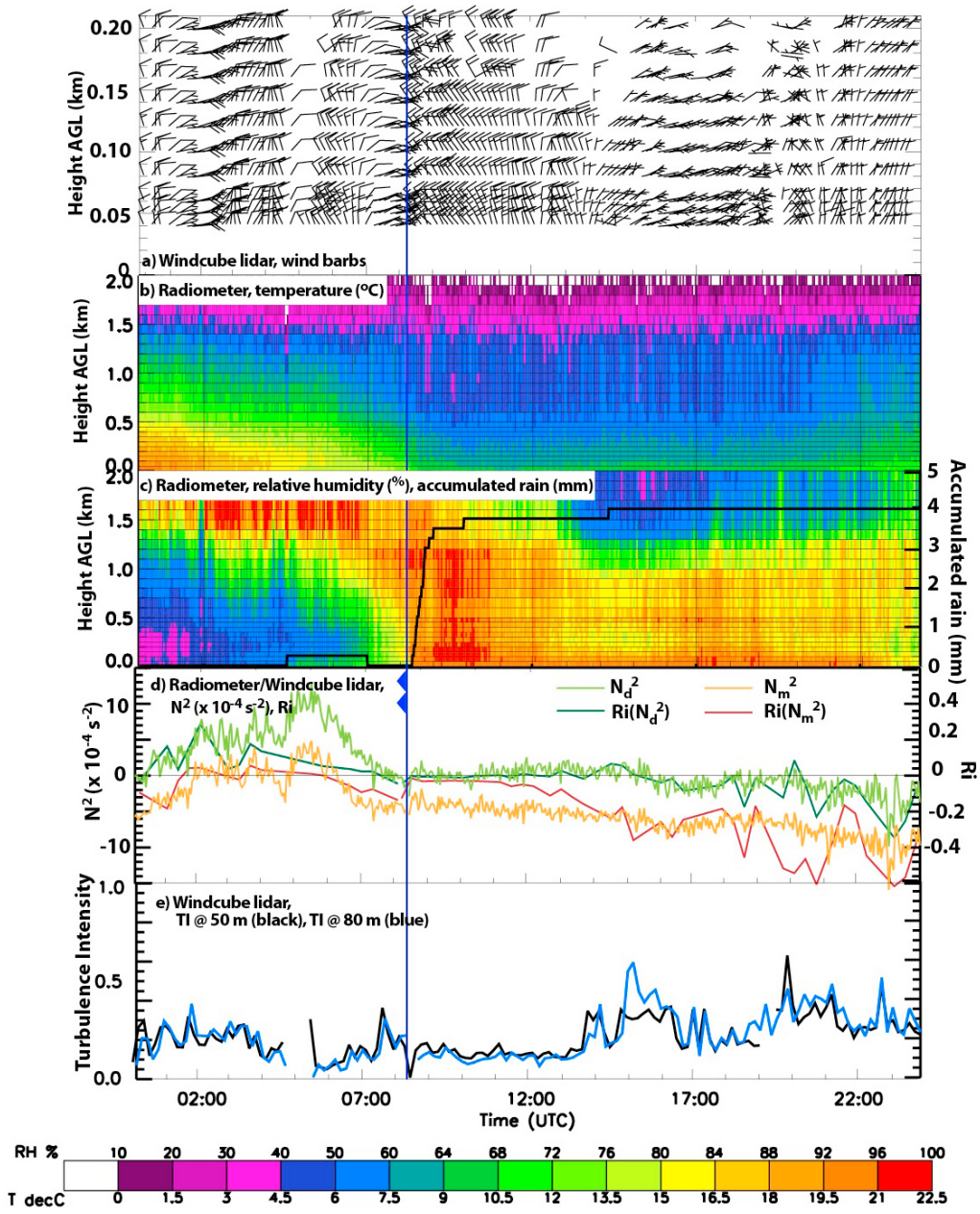

Figure 3. Windcube lidar and microwave observations on 9 June 2011 during a cold front passage. (a) winds (half barb is 2.5 m s^{-1} and full barb is 5 m s^{-1}) observed by the Windcube lidar, (b, c) temperature and relative humidity observed by the microwave radiometer, (d) N_d^2 and N_m^2 between the surface and 50 m AGL derived from radiometer observations and *Ri* derived from the Windcube and radiometer measurements, and (e) turbulence intensity derived from the Windcube lidar at 50 m and 80 m AGL. The location of the surface cold front is shown as a blue line with filled triangle symbols attached. Rain was occasionally observed by the radiometer rain sensor in Figure 3c.

humidity profile on atmospheric stability and Richardson number.

[14] The Windcube lidar and Radiometrics microwave radiometer provided temperature and wind speed measurements as accurate as the *in-situ* tower observations. Differences in temperature ranged between 0.7–1.7°C between the tower and radiometer. Slightly larger values were observed at the surface, which were likely related to thermal turbulence rather than instrument accuracy. Wind observations from the Windcube lidar and *in-situ* tower indicated a spread of 1.2 ms^{-1} for wind speed. As a result, the differences in squared Brunt-Väisälä frequency and the Richardson numbers based on *in-situ* tower and remote sensing observations showed median values of 0.2×10^{-4} s^{-2} and 0.013 and spread values of 3.2×10^{-4} s^{-2} and 0.13, respectively.

[15] While the importance of humidity measurements has yet to be established for wind energy applications, we demonstrated that the atmospheric stability, and therefore *Ri*, were determined more accurately when the liquid-water mixing ratio derived from the vertical humidity profile was considered in a saturated atmosphere. Under those conditions, N_m^2 derived from the radiometer humidity profile

indicated that the atmosphere was unstable, instead of stable as indicated when using N_d^2. In those cases, changes in the squared Brunt-Väisälä frequency affected the accuracy of *Ri* and therefore, the relationship between the *Ri* and the turbulence intensity.

[16] This comparison study also showed the ability of the remote sensing instruments in overcoming the limits of traditional tower measurements by measuring wind, temperature and humidity beyond 100 m AGL. In addition, the small footprint of the remote sensing instruments provides flexibility in choosing deployment locations. Wind measurements and, therefore, the calculation of *Ri,* are not limited to cases when the orientation of an anemometer is appropriate for the wind direction but can instead be accomplished under any wind direction. Further observational studies are necessary to quantify the role of vertical humidity profiles on the stability during moist-adiabatic conditions and to determine how humidity impacts the formation and maintenance of low-level wind maxima and wind turbine performance.

[17] **Acknowledgments.** The Editor thanks the two anonymous reviewers for their assistance in evaluating this paper.

References

Aitken, M., M. E. Rhodes, and J. K. Lundquist (2012), Performance of a wind-profiling lidar in the region of wind turbine rotor disks, *J. Atmos. Oceanic Technol.*, doi:10.1175/JTECH-D-11-00033.1, in press.

AWS Truepower (2010), Wind resource assessment handbook, *Final Rep. 10–30*, N. Y. State Energy Res. and Dev. Auth., Albany. [Available at http://www.awstruepower.com/2010/10/nyserda-aws-truepower-publish-wind-resource-assessment-handbook-2010/.]

Colle, B. A., J. B. Wolfe, W. J. Steenburgh, D. E. Kingsmill, J. A. W. Cox, and J. C. Shafer (2005), High-resolution simulations and microphysical validation of an orographic precipitation event over the Wasatch Mountains during IPEX IOP3, *Mon. Weather Rev.*, *133*, 2947–2971, doi:10.1175/MWR3017.1.

Durran, D. R., and J. B. Klemp (1982), On the effects of moisture on the Brunt-Väisälä frequency, *J. Atmos. Sci.*, *39*, 2152–2158, doi:10.1175/1520-0469(1982)039<2152:OTEOMO>2.0.CO;2.

Einaudi, F., and D. P. Lalas (1973), On the correct use of the wet adiabatic lapse rate in stability criteria of a saturated atmosphere, *J. Appl. Meteorol.*, *13*, 318–324.

Kaiser, K., H. Hohlen, and W. Langreder (2003), Turbulence correction for power curves, paper presented at the 2003 European Wind Energy Conference, Eur. Wind Energy Assoc., Madrid, 16–19 June.

Mahrt, L. (2010), Variability and maintenance of turbulence in the very stable boundary layer, *Boundary Layer Meteorol.*, *135*, 1–18, doi:10.1007/s10546-009-9463-6.

Rareshide, E., A. Tindal, C. Johnson, A. Graves, E. Simpson, J. Bleeg, T. Harris, and D. Schoborg (2009), Effects of complex wind regimes on turbine performance, paper presented at the WINDPOWER 2009, Am. Wind Energy Assoc., Chicago, Ill., 4–7 May.

Steenburgh, W. J. (2003), One hundred inches in one hundred hours: Evolution of a Wasatch Mountain winter storm cycle, *Weather Forecast.*, *18*, 1018–1036, doi:10.1175/1520-0434(2003)018<1018:OHIIOH>2.0.CO;2.

Vanderwende, B., and J. K. Lundquist (2012), The Effects of atmospheric stability and wind shear on wind farm power production, *Wind Energy*, in press.

Vickers, D., and L. Mahrt (2004), Evaluating formulations of stable boundary layer height, *J. Appl. Meteorol.*, *43*, 1736–1749, doi:10.1175/JAM2160.1.

Wharton, S., and J. K. Lundquist (2012), Atmospheric stability impacts on power curves of wind turbines—An analysis of a West Coast North American wind farm, *Environ. Res. Lett.*, in press.

M. Aitken, Department of Physics, University of Colorado at Boulder, 390 UCB, Boulder, CO 80309-0390, USA.

K. Friedrich, E. A. Kalina, J. K. Lundquist, and R. F. Marshall, Department of Atmospheric and Oceanic Sciences, University of Colorado at Boulder, 311 UCB, Boulder, CO 80309-0311, USA. (katja.friedrich@colorado.edu)